Available online at www.sciencedirect.com
SCIENCE DIRECT
Journal of the European Ceramic Society 26 (2006) 1287–1292
www.elsevier.com/locate/jeurceramsoc

Interface structure and mechanical properties of the brazed joint of TiC cermet and steel

Jicai Feng, Lixia Zhang *

National Key Laboratory of Advanced Welding Production Technology, Harbin Institute of Technology, Harbin 150001, China

Received 11 September 2004; received in revised form 13 January 2005; accepted 23 January 2005
Available online 2 March 2005

Abstract

A commercially available Ag–Cu braze alloy foil with Zn was used to join TiC cermet and steel. According to the experimental observations, the interface structure is (Cu, Ni)/Ag (s.s.) + Cu (s.s.)/(Cu, Ni)/(Cu, Ni) + (Fe, Ni) from TiC cermet to steel side. With increased brazing temperature or time, the amounts of (Cu, Ni) near the base metals/Ag–31Cu–23Zn interface and (Cu, Ni) + (Fe, Ni) near the Ag–31Cu–23Zn/steel interface increase, while the amount of Ag (s.s.) + Cu (s.s.) in the middle of the braze alloy decreases. The whole joining process consists of diffusion and solution among atoms of the braze alloy foil and base metals. The maximum shear strength is 120.7 MPa for the joint brazed at 850 °C for 10 min.

Keywords: TiC cermet; Joining; Interfaces; Microstructure; Strength

1. Introduction

In the last few years, materials formed by ceramics and metallic phases ("cermets") have received increasing attention because of their singular mechanical, electrical and magnetic properties.[1] These cermets have been proposed as excellent candidates for structural and high added-value functional applications related to aerospace industry, energy conversion, sensors and transductors.[2] Most metal-matrix cermets, especially those reinforced by ceramics, can be produced economically by a combustion synthesis process, sometimes called self-propagating high-temperature synthesis (SHS), which provides an attractive affordable alternative to the conventional methods of producing advanced materials.[3–6]

As a new type of material, TiC cermet synthesized by SHS has great potential to become an important candidate for advanced application owing to its high hardness, excellent wear resistance and high elevated-temperature strength.[7] The major constituents of TiC cermet consist of TiC particles, which are hard and brittle, and the minor constituent binder metal Ni, which is relatively soft and ductile.

To expand the practical applications of the cermets, it is necessary to bond them to metals. Now, the research on the bonding technologies of ceramics to metals is well documented, such as brazing,[8–13] diffusion bonding,[14,15] microwave welding[16] and ultrasonic welding.[17] Of them, brazing has become one of the main methods of bonding ceramics to metals. However, to braze ceramics to metals successfully, it has to face two challenges. Most of the metals have poor wettability with ceramics. The most convenient method to resolve this is to use active filler metal for brazing ceramics and metals. Previous studies and comprehensive reviews have been published in this area.[18–23] The other challenge of brazing ceramic to metal rests with accommodating the thermal expansion mismatch between ceramics and metals, and minimizing the resulting residual stresses.

It is well-known that Ag-based braze alloys are widely used to braze most ceramics. Especially, the utilization of a Ag-base braze alloy with Zn can improve the wetting and spreading on the surface of ceramics, and the disadvantageous effects of Zn on corrosion resistance of the joint can be reduced by the evaporation of Zn after the braze alloy

* Corresponding author. Tel.: +86 45186418882; fax: +86 45186413951.
E-mail address: zhanglxia@hit.edu.cn (L. Zhang).

0955-2219/$ – see front matter © 2005 Elsevier Ltd. All rights reserved.
doi:10.1016/j.jeurceramsoc.2005.01.043

Table 1
Chemical content of steel (wt.%)

Elements	Contents
C	0.43
Si	0.34
Mn	0.41
Cr	0.10
P	0.03
S	0.06
Al	1.57
Fe	Remains

melts in the vacuum circumstances. The current investigation concentrates on the joining of TiC cermet and steel using Ag–31Cu–23Zn braze alloy. The interface structure, interface evolution mechanism, and shear strength are comprehensively studied to access the relation between the microstructure and the joint performance.

2. Experiment procedures

The cermet material used in the experiments was TiC cermet, the content of which was 60 wt.% TiC and 40 wt.% Ni. Commercially obtained Ag–31Cu–23Zn (wt.%) braze alloy (thickness 120 μm) and steel were used in the test. The chemical content of the steel is shown in Table 1. The microstructure of TiC cermet and steel are shown in Fig. 1.

The size of the brazed specimens was 40 mm × 10 mm × 5 mm. TiC cermet and steel were overlapped for 8 mm along the length of the specimens (see Fig. 2a). All joined surfaces were polished by SiC papers up to grit 1200, and cleaned in ethanol and acetone prior to vacuum brazing. The stacked TiC cermet/Ag–31Cu–23Zn/steel assembly was brazed in a vacuum furnace (Centorr-3520) equipped with a hydraulic system. Vacuum brazing was performed in a vacuum of 6.6 MPa, and the heating and cooling rate was, respectively, set at 30 °C/min and 20 °C/min.

After brazing, shear tests were performed by an Instron-1186 mechanical testing machine to evaluate the shear strength of the vacuum brazed joints (see Fig. 2a). The brazed specimens were stretched by a universal testing machine with a constant speed of 1 mm/min. To observe the cross section of the brazed specimens, the brazed joints were cut to 10 mm × 5 mm × 1 mm (see Fig. 2b). The cross section of the joints was polished using 0.5 μm diamond paste as final polish and cleaned in acetone. The nano-indenter hardness of the brazed joint was measured by Nano-Indenter XP machine. The cross section of the brazed specimens was examined using S-4700 scanning electron microscope (SEM) equipped with an energy dispersive spectrometer (EDS) and an electron probe X-ray microanalysis (EPMA).

3. Results and discussion

3.1. Interface structure of the brazed TiC cermet/Ag–31Cu–23Zn/steel joint

Fig. 3 shows the back-scattered electron image and major element content distributions (along the line indicated in the electron image) of TiC cermet/steel joint brazed with Ag–31Cu–23Zn braze alloy foil at 850 °C for 15 min. It can be seen from the image that there are three zones between the TiC cermet and the steel. For the sake of convenience, the irregular dark blocks adjacent to the TiC cermet and the steel are, respectively, called A and C zones, and the zone between the A and C zones is called B zone, which is composed of duplex phases (black strips and white phases) and the white

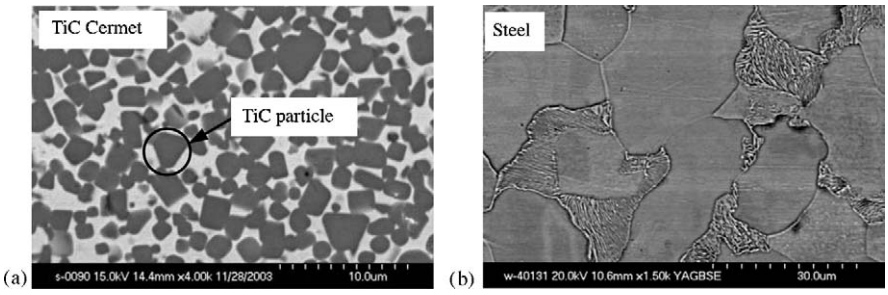

Fig. 1. Microstructure of base metals: (a) TiC cermet and (b) steel.

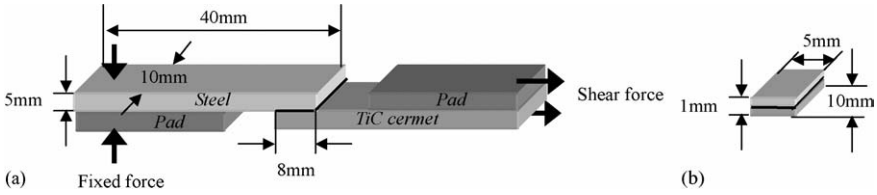

Fig. 2. Size of the TiC cermet/Ag–31Cu–23Zn/steel joint: (a) shear testing sample and (b) metallographic analysis sample.

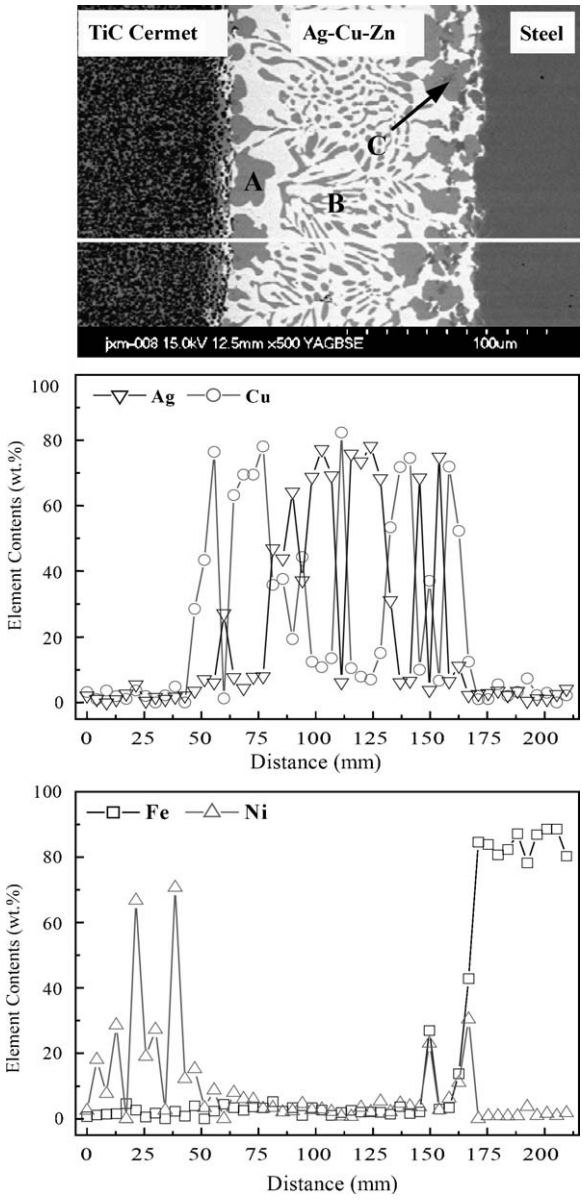

Fig. 3. Back-scattered electron image and major element content distribution of TiC cermet/steel joint brazed with Ag–31Cu–23Zn at 850 °C for 15 min.

Table 2
Average chemical compositions of each zone on the brazed joint (wt.%)

Zones	Chemical composition (wt.%)						
	Ag	Cu	Fe	Ni	C	Zn	Ti
A	3.32	83.62	1.44	5.35	3.01	3.03	0.22
B (white phases)	69.17	18.44	1.77	1.57	4.69	3.77	0.59
B (black stripes)	20.22	74.17	0.38	0.22	2.70	1.90	0.41
C	3.00	78.85	2.82	9.79	3.09	2.20	0.25
D	1.85	9.95	56.11	26.36	5.01	0.72	0.00
E	1.28	39.46	28.57	24.23	4.16	1.96	0.35

phases are matrixes. It can be shown from major element content distributions that the A and C zones are Cu-rich zones. Meanwhile, the black strips in the B zone are also Cu-rich and the white phases in the B zone are Ag-rich. Because the concentration profiles of the major elements in Fig. 3 fluctuate in the A–C zones, there are perhaps not compounds but solid solutions occurred in these three zones.

To see the brazed joint clearly, it is necessary to show the microstructure of TiC cermet/Ag–31Cu–23Zn interface and Ag–31Cu–23Zn/steel interface in Fig. 4. It can be observed from Fig. 4(a) that some TiC particles float from the TiC cermet into the A zone during brazing at the TiC cermet/Ag–31Cu–23Zn interface, which shows that Ag–31Cu–23Zn braze alloy has good wetting capability on the surface of the TiC cermet. It can be seen from Fig. 4(b) that there occurs a new irregular dark layer (named D zone) on the Ag–31Cu–23Zn/steel interface, meanwhile there are some dispersedly distributed dark phases (named E zone) between C and D zones. Thus, the TiC cermet/steel joint brazed with Ag–31Cu–23Zn braze alloy at 850 °C for 15 min can be divided into five zones, A, B, C, D and E, respectively.

Table 2 gives the average chemical compositions of each zone of the TiC cermet/steel joint brazed at 850 °C for 15 min. It can be seen from Table 2 that there are much Cu and a little Ni in the A and C zones. Because Ni–Cu is infinity solid solution system according to the Ni–Cu phase diagram, there exists (Cu, Ni) solid solution in these two zones. The dark strips of B zone are composed of much Cu and a little Ag, so there is Cu-base solid solution (namely Cu (s.s.)). At the same time, the white phases of B zone consist of much Ag and a little Cu, so there is Ag-base solid solution (namely Ag (s.s.)). According to the Ag–Cu phase diagram, it is well

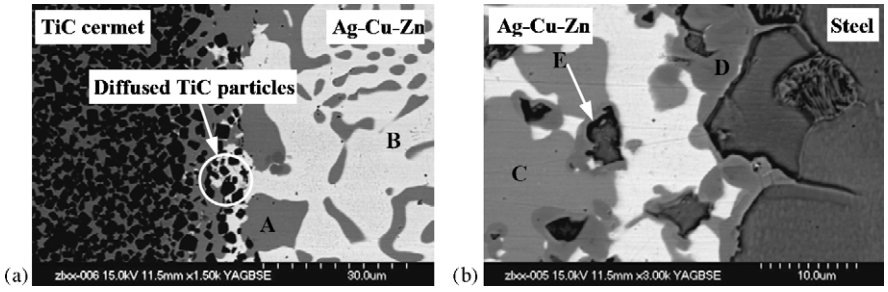

Fig. 4. Microstructure of the TiC cermet/Ag–31Cu–23Zn/steel interface brazed at 850 °C for 15 min: (a) TiC cermet/Ag–31Cu–23Zn interface and (b) Ag–31Cu–23Zn/steel interface.

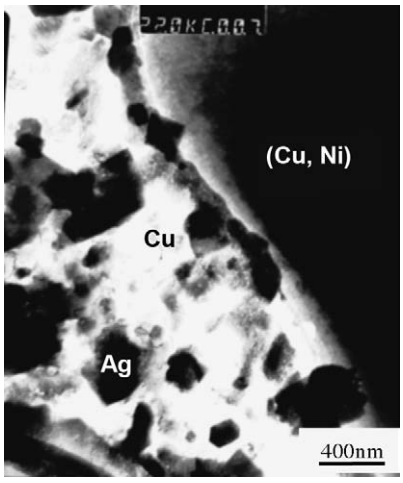

Fig. 5. TEM image showing the interface morphology of Ag (s.s.)+Cu (s.s.) and (Cu, Ni) solid solution zones.

known that the B zone is a eutectic structure composed of Cu (s.s.) and Ag (s.s.). Fig. 5 is TEM image showing the interface morphology of B and C zones, from which it can be clearly seen that Ag (s.s.) + Cu (s.s.) and (Cu, Ni) solid solutions, respectively, exist in the B and C zones.

It also can be seen from Table 2 that there are a lot of Fe and a little Cu and Ni in the D zone, meanwhile there are a lot of Cu and a little Fe and Ni in the dispersedly distributed dark phases (E zone). According to Fe–Cu–Ni ternary phase diagram, there are (Cu, Ni) solid solution and (Fe, Ni) solid solution occurred in D and E zones. Thus, these five zones are, respectively (Cu, Ni), Ag (s.s.) + Cu (s.s.), (Cu, Ni), (Cu, Ni) + (Fe, Ni) and (Cu, Ni) + (Fe, Ni) from A to E zone.

Table 3
Nano-indenter hardness of each zone on TiC cermet/steel joint

Zones	A	B		C	D
		Ag (s.s.)	Cu (s.s.)		
Hardness (GPa)	2.638	1.817	1.673	2.542	3.806

3.2. The interface evolution mechanism of the brazed TiC cermet/Ag–31Cu–23Zn/steel joint

Fig. 6 displays the interface evolution model for the TiC cermet/steel joint brazed with Ag–31Cu–23Zn. As indicated in Fig. 6, the whole reaction process can be divided into three stages. In the first stage, when the brazing temperature is up to the melting point of Ag–31Cu–23Zn braze alloy, it melts and becomes liquid. In this stage, a little Ni in TiC cermet and a little Fe in steel diffuse to the braze alloy. At the same time, some TiC particles float onto the interface of TiC cermet/Ag–31Cu–23Zn. With the increased brazing temperature, a little Cu and Ag move freely in the braze alloy. In the second stage, when the brazing temperature begins to decline, (Cu, Ni) and (Cu, Ni) + (Fe, Ni) occur on the interface of Ag–31Cu–23Zn/steel. At the same time, there is (Cu, Ni) at the interface of TiC cermet/Ag–31Cu–23Zn. In the third stage, with the declining of the brazing temperature,

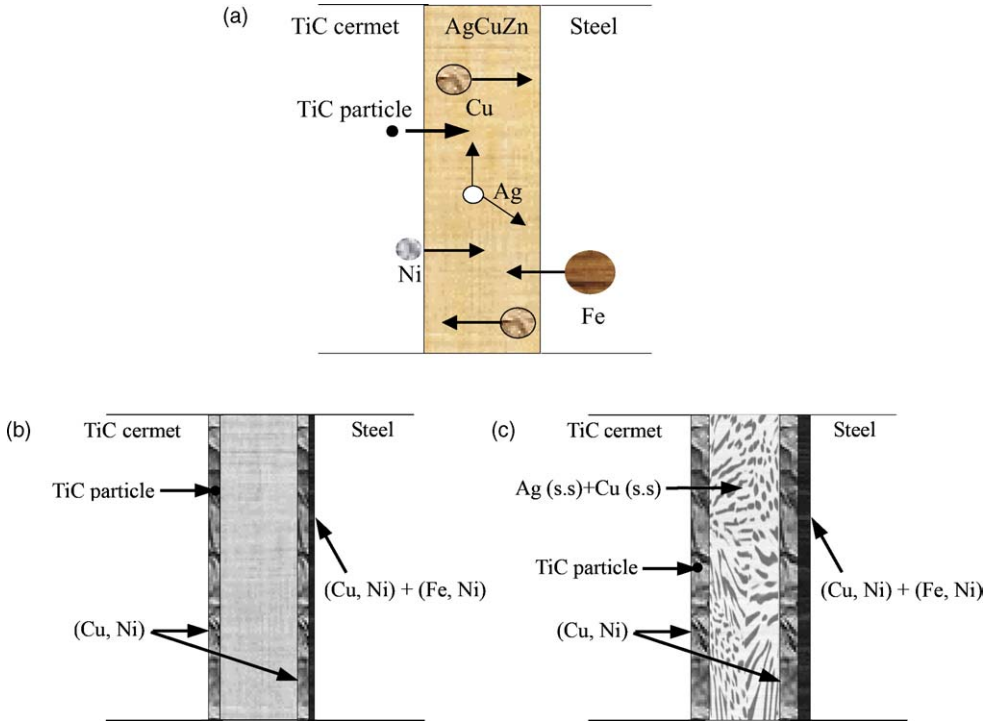

Fig. 6. Interface evolution model for the TiC cermet/steel joint brazed with Ag–31Cu–23Zn: diffusion (a) and solution (b and c).

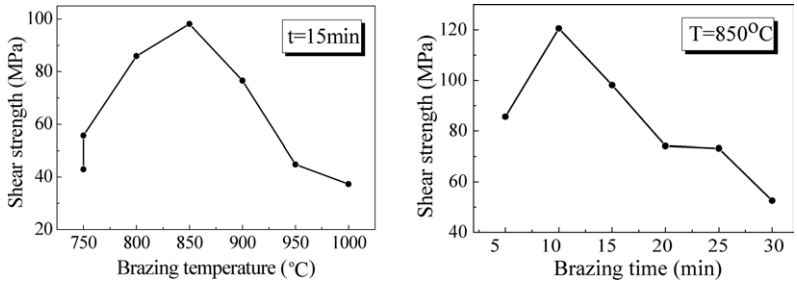

Fig. 7. Shear strength of the TiC cermet/Ag–31Cu–23Zn/steel joint brazed: (a) at different temperatures for 15 min and (b) at 850 °C for different time periods.

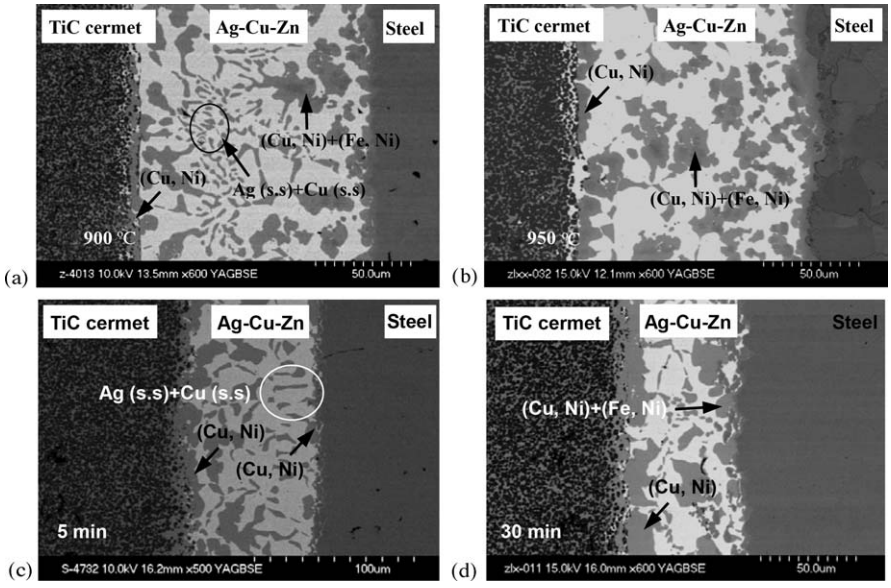

Fig. 8. Microstructure of the TiC cermet/Ag–31Cu–23Zn/steel joint brazed for 15 min (a and b) and at 850 °C (c and d).

the amounts of (Cu, Ni) and (Cu, Ni) + (Fe, Ni) increase at the interface of Ag–31Cu–23Zn/base metals. Meanwhile, there appear a lot of eutectic stripes in the braze alloy. Finally, the interface structure of the joint is TiC cermet/(Cu, Ni)/Ag (s.s.) + Cu (s.s.)/(Cu, Ni)/(Cu, Ni) + (Fe, Ni)/steel from TiC cermet to steel side.

3.3. Mechanical evaluation of the brazed TiC cermet/Ag–31Cu–23Zn/steel joint

Fig. 7 shows the shear strength of the joints brazed at different temperatures for 15 min and at 850 °C for different time periods. It can be known from Fig. 7 that when the brazing temperature is low or brazing time is short, the shear strength of the joints is not satisfactory. Further increasing the brazing temperature or time will result in the appearance of the maximum shear strength values. Based on Fig. 7, the maximum shear strength of the joint is 120.7 MPa obtained at 850 °C for 10 min.

Table 3 gives the nano-indenter hardness of formation products in the TiC cermet/steel joint brazed at 850 °C for 15 min. According to the experimental results, Ag (s.s.) + Cu (s.s.) is soft compared with other products and (Cu, Ni) + (Fe, Ni) in D zone demonstrates the highest hardness phase in the joint.

From the microstructural point of view, the change of the shear strength is due to the amount changes of (Cu, Ni), Ag (s.s.) + Cu (s.s.) and (Cu, Ni) + (Fe, Ni) phases as the brazing temperature or time increases. Fig. 8 shows the microstructure of TiC cermet/Ag–31Cu–23Zn/steel interface brazed at 900 °C or 950 °C for 15 min, and at 850 °C for 5 or 30 min. It can be known from Fig. 8 and chemical composition analysis, when the brazing temperature is up to 900 °C or the brazing time is up to 30 min, there is no (Cu, Ni) zone but (Cu, Ni) + (Fe, Ni) zone on the interface of Ag–31Cu–23Zn/steel. Especially, when the brazing temperature is up to 950 °C, Cu (s.s.) stripes in B zone have disappeared and there are a lot of (Cu, Ni) + (Fe, Ni) phases in the braze alloy. Therefore, the amount of (Cu, Ni) + (Fe, Ni) increase, while that of Ag (s.s.) + Cu (s.s.) decreases with the increased brazing temperature or prolonged brazing time. Because these formation products have different hardness value, whose amount changes can lead to the appearance of maximum shear strength value.

4. Conclusions

According to the experimental observation, there exist (Cu, Ni), Ag (s.s.) + Cu (s.s.), (Cu, Ni), (Cu, Ni) + (Fe, Ni) zones on TiC cermet/Ag–31Cu–23Zn/steel joint. The whole interface evolution process can be divided into three stages. The diffusion of atoms exists in the first stage and solid solution of atoms appears in the second and third stages. With the increased brazing temperature or time, the amount of (Cu, Ni) + (Fe, Ni) increases, while the amount of Ag (s.s.) + Cu (s.s.) decreases. The maximum shear strength is 120.7 MPa for the joint brazed at 850 °C for 10 min.

Acknowledgement

This work was supported by the National Natural Foundation of Science (No. 50325517), People's Republic of China.

References

1. Rodrigurez, A. M., Leon, A. B., Rodrigurez, A. D., Esteban, S. L., Moya, J. S. and Melendo, M. J., High-temperature mechanical properties of zirconia/nickel composites. *J. Eur. Ceram. Soc.*, 2003, **23**, 2849–2856.
2. Reschke, S. and Bodganow, C., Engineering ceramics: new perspectives through value-added (multi-) function. *Key Eng. Mater.*, 1999, **175/176**, 1–10.
3. Xiao, G. Q., Fan, Q. C., Gu, M. Z., Wang, Z. H. and Jin, Z. H., Dissolution-precipitation mechanism of self-propagating high-temperature synthesis of TiC–Ni cermet. *Mater. Sci. Eng. A*, 2004, **382**, 132–140.
4. Fu, Z. Y., Wang, H., Wang, W. M. and Yuan, R. Z., Composites fabricated by self-propagating high-temperature synthesis. *J. Mater. Process. Technol.*, 2003, **137**, 30–34.
5. Zhang, X. H., He, X. D. and Han, J. C., Self-propagating high temperature combustion synthesis of TiB/Ti composites. *Mater. Sci. Eng. A*, 2003, **348**, 41–46.
6. Zhang, X. H., He, X. D., Han, J. C., Qu, W. and Kvalin, V. L., Combustion synthesis and densification of large-scale TiC–*x*Ni cermets. *Mater. Lett.*, 2002, **56**, 183–187.
7. Han, J. C., Zhang, X. H. and Wood, J. V., In-situ combustion synthesis and densification of TiC-xNi. *Mater. Sci. Eng. A*, 2000, **280**, 328–333.
8. Rice, J. P., Paxton, D. M. and Weil, K. S., Oxidation behavior of a commercial gold-based braze alloy for ceramic-to-metal joining. *Ceram. Eng. Sci. Proc.*, 2002, **23**, 809–816.
9. Yoo, Y. C., Kim, J. H. and Park, K., Microstructural characteriazation of Al_2O_3/AISI 8650 steel joint brazed with Ag–Cu–Sn–Zr alloy. *Mater. Lett.*, 2000, **42**, 362–366.
10. Zhang, C. G., Qiao, G. J. and Jin, Z. H., Active brazing of pure alumina to kovar alloy based on the partial transient liquid phase (PTLP) technique with Ni-Ti interlayer. *J. Eur. Ceram. Soc.*, 2002, **22**, 2181–2186.
11. Durov, A. V., Kostjuk, B. D. and Shevchenko, A. V., Joining of zirconia to metal with Cu–Ga–Ti and Cu–Sn–Pb–Ti fillers. *Mater. Sci. Eng. A*, 2000, **290**, 186–189.
12. Vianceo, P. T., Stephens, J. J., Hlava, P. F. and Walker, C. A., Titanium scavenging in Ag–Cu–Ti active braze joints. *Weld. Res.*, 2003, **82**, 268–277.
13. Chaumat, G., Drevet, B. and Vernier, L., Reactive brazing study of a silicon nitride to metal joining. *J. Eur. Ceram. Soc.*, 1997, **17**, 1925–1927.
14. Kliauga, A. M., Travessa, D. and Ferrante, M., Al_2O_3/Ti interlayer/AISI 304 diffusion bonded joint: microstructural characterization of the two interfaces. *Mater. Charact.*, 2001, **46**, 65–74.
15. Travessa, D., Ferrantem, M. and Den, O. G., Diffusion bonding of aluminium oxide to stainless steel using stress relief interlayers. *Mater. Sci. Eng. A*, 2002, **337**, 287–296.
16. Siores, E. and Rego, D. D., Microwave applications in materials joining. *J. Mater. Process. Technol.*, 1995, **48**, 619–625.
17. Matsuoka, S. I., Ultrasonic welding of ceramics/metals using inserts. *J. Mater. Process. Technol.*, 1998, **75**, 259–265.
18. Elsawy, A. H. and Fahmy, M. F., Brazing of Si_3N_4 ceramic to copper. *J. Mater. Process. Technol.*, 1998, **77**, 266–272.
19. Sciti, D., Bellosi, A. and Esposito, L., Bonding of zirconia to super alloy with the active brazing technique. *J. Eur. Ceram. Soc.*, 2001, **21**, 45–52.
20. Qiao, G. J., Zhang, C. G. and Jin, Z. H., Thermal cyclic test of alumina/kovar joint brazed by Ni–Ti active filler. *Ceram. Int.*, 2003, **29**, 7–11.
21. Arroyave, R. and Eagar, T. W., Metal substrate effects on the thermochemistry of active brazing interfaces. *Acta Mater.*, 2003, **51**, 4871–4880.
22. Brochu, M., Pugh, M. D. and Drew, R. A. L., Joining silicon nitride ceramic using a composite powder as active brazing alloy. *Mater. Sci. Eng. A*, 2004, **374**, 34–42.
23. Hanson, W. B., Ironside, K. I. and Fernie, J. A., Active metal brazing of zirconia. *Acta Mater.*, 2000, **48**, 4673–4676.